

Adinkras From Ordered Quartets of BC₄ Coxeter Group Elements and Regarding Another Gadget's 1,358,954,496 Matrix Elements

S. James Gates, Jr.,^{1a} Lucas Kang,^{2a} David S. Kessler,^{3b} and Vadim Korotkikh^{4c}

^a*Department of Physics, Brown University,
Box 1843, 182 Hope Street, Barus & Holley 545, Providence, RI 02912, USA*

^b*Amherst Center for Fundamental Interactions, Department of Physics,
University of Massachusetts, Amherst, MA 01003, USA*

and

^c*Department of Physics, University of Maryland,
4150 Campus Dr., College Park, MD 20472, USA*

ABSTRACT

A Gadget, more precisely a scalar Gadget, is defined as a mathematical calculation acting over a domain of one or more adinkra graphs and whose range is a real number. A 2010 work on the subject of automorphisms of adinkra graphs, implied the existence of multiple numbers of Gadgets depending on the number of colors under consideration. For four colors, this number is two. In this work, we verify the existence of a second such Gadget and calculate (both analytically and via explicit computer-enabled algorithms) its 1,358,954,496 matrix elements over 36,864 minimal valise adinkras related to the Coxeter Group BC₄.

PACS: 11.30.Pb, 12.60.Jv

Keywords: quantum mechanics, supersymmetry, off-shell supermultiplets

¹ gatess@wam.umd.edu

² lucas_kang@brown.edu

³ 3.14159.david@gmail.com

⁴ va.korotki@gmail.com

1 Introduction

Our study of “Garden Algebras” [1,2] and “adinkras” [3] has opened multiple pathways for understanding the relation of supersymmetry, in most unexpected ways, to topics in mathematics. Such a demonstration appeared in the recent examples [4,5] connecting adinkras to algebraic geometry as the latest following a host of others [6,7,8,9,10,11,12,13].

As adinkras are bipartite graphs, this opens access to methods (e.g. [14]) associated with graph theory [15,16,17,18,19] as an additional tools to study supersymmetry theory. Indeed, there is a enormously large and rapidly expanding literature that emphasizes the importances of networks and graphs across fields as diverse as biology, chemistry, computer science, engineering, medicine, neuroscience, and physics as noted in the work of [20]. This has prompted at least one call to identify all this activity as heralding the emergence of a new field called “network science” [21]. From this vantage, the study of adinkras constitutes a network scientific approach to the study of the representation theory of spacetime supersymmetry.

In a previous work [22] motivated by Garden Algebras and adinkras, an information technology (IT) computer-enabled algorithm was applied to the Coxeter Group BC_4 [23] which contains $384 = 4! \times 2^4$ elements that each describes a signed permutation. The result of this application was it provided a calculational proof of a previously unknown mathematical theorem. The Coxeter Group BC_4 can be regarded as the union of 96 disjoint “tetrads,” subsets $\hat{q}_{[1]} \cdots \hat{q}_{[96]}$, i. e.

$$BC_4 = \hat{q}_{[1]} \cup \hat{q}_{[2]} \cup \cdots \cup \hat{q}_{[96]} = \prod_{i=1}^{96} \hat{q}_{[i]} \quad , \quad (1.1)$$

where each tetrad defines a 1D, $N = 4$ supersymmetry representation as the tetrad elements $\{\mathbf{L}_1, \mathbf{L}_2, \mathbf{L}_3, \mathbf{L}_4\}$ can be chosen to satisfy the Garden Algebra. An obvious question raised by this result is whether and how does it extend to other Coxeter Groups?

Given a specified tetrad with elements $\{\mathbf{L}_1, \mathbf{L}_2, \mathbf{L}_3, \mathbf{L}_4\}$, by considering all possible replacements $\mathbf{L}_I \rightarrow \pm \mathbf{L}_I$ for any fixed value of the subscript I , one obtains $2^4 = 16$ other tetrads. We call this type of replacement a “flip” of the tetrad. Also given the specific tetrad one can re-order the elements within the tetrad. As each tetrad contains four elements, there are $4! = 24$ such re-orderings. We refer to such re-orderings as “flops.” Taking the flips and flops together, we realize that they constitute another realization of the the Coxeter Group BC_4 ! When the ordering of the elements in tetrads is important that also increases the number of possibilities. In the work of [24], it was shown how to use a bi-quaternionic basis together with the flips, and the flops, to efficiently describe this large system of possibly independent representations.

By these arguments, one can conclude there are a maximum of $4! \times 2^4 \times 96 = 36,864$ 1D, $N = 4$ valise supersymmetry representations related to the Coxeter Group BC_4 . It is therefore useful to introduce an index that indicates which of these 36,864 representations we wish to specify. This is done by using a notation $\mathbf{L}_I^{(\mathcal{R})}$ (when necessary) where the index (\mathcal{R}) (called the “representation label”) takes on values of $1, \dots, 36,864$. This number can be reduced. For example, if $\hat{q}_{[i]} = -\hat{q}_{[j]}$ with $i \neq j$, the two tetrads can be said to describe the same representation for many purposes.

While the valise adinkra representation index (\mathcal{R}) takes on values from one to 36,864 for the minimal BC_4 valise adinkras, until recently the range of this index for adinkras with more colors and/or more nodes was not known. A recent work by Zhang [25] has presented a theorem that determines the equivalent number to 36,864 for any valise adinkra with d nodes (open and closed) and N colors where both d and N are arbitrary positive integers.

As was noted in the work of [26], 4D, Lorentz symmetry and $\mathcal{N} = 1$ supersymmetry, determine the number of minimal off-shell representations to be ten. By use of 4D Hodge duality, this number can be reduced to five. These five representations “live” in a four dimensional “weight space-like” setting characterized by four integers $p_{(\widehat{\mathcal{R}})}$, $q_{(\widehat{\mathcal{R}})}$, $r_{(\widehat{\mathcal{R}})}$, and $s_{(\widehat{\mathcal{R}})}$. If one assigns a Euclidean metric for these coordinates, the supermultiplets in the weight-like space all reside on the surface of a four dimensional unit sphere.

One of the 4D, $\mathcal{N} = 1$ supermultiplets lives on the $s_{(\widehat{\mathcal{R}})}$ -axis. We can think of this supermultiplet along the $s_{(\widehat{\mathcal{R}})} \neq 0$ as sitting at the apex of a pyramid which has a square as its base. The remaining four supermultiplets live in a three-space orthogonal to the $s_{(\widehat{\mathcal{R}})}$ -axis with one of each of the supermultiplets at half of the vertices of a tetrahedron.

Of the four supermultiplets located at half of the vertices of the tetrahedron, two are related to one another via parity exchanges of their coordinates according to $p_{(\widehat{\mathcal{R}})} \rightarrow -p_{(\widehat{\mathcal{R}})}$ and $q_{(\widehat{\mathcal{R}})} \rightarrow -q_{(\widehat{\mathcal{R}})}$. So in a sense there are only three minimal 4D, $\mathcal{N} = 1$ supermultiplets which we may call the “chiral supermultiplet” (the one with $s_{(\widehat{\mathcal{R}})} \neq 0$), the “vector supermultiplet” and the “tensor supermultiplet” (these two along with their parity doubles reside at the vertices of a tetrahedron).

Theories that possess 4D, $\mathcal{N} = 1$ spacetime supersymmetry can, via various reduction techniques, yield 1D, $N = 4$ theories. We have used this fact to create a method [27,28] for extracting the Garden Algebras and associated adinkras for any four dimensional supermultiplet. Use of such reduction procedures lead from the three 4D, $\mathcal{N} = 1$ supermultiplets to three adinkras along with their tetrads...among a sea of 36,864 possible adinkras. So the question is which adinkras are selected? The answer to this depends on the conventions used to write the 4D, $\mathcal{N} = 1$ spacetime supermultiplet as well as the details of the conventions used in the reduction.

It has been long our suggestion that one should identify an equivalence class among the adinkras so that the choice of conventions used to write the 4D, $\mathcal{N} = 1$ spacetime supermultiplet as well as the details of the conventions used in the reduction are irrelevant to all members in the equivalence class. Thus, one is faced with the issue of defining these classes. This is where the notion of 4D, $\mathcal{N} = 1$ “Gadgets” enter.

Owing to the fact that supercharges transform bosons into fermions and vice-versa, the notion of an eigenfunction or eigenvector for the supercharges cannot be defined. As the usual path to roots and weights of representations precedes along with the concepts of eigenvectors and eigenvalues, this route cannot be traversed here. In the works of [26,29], it was shown that operators quadratic in the supercharges when evaluated on the fermionic fields of the supermultiplets allow for the emergence of numbers that can play the role of the eigenvalues. These are precisely the four integers $p_{(\widehat{\mathcal{R}})}$, $q_{(\widehat{\mathcal{R}})}$, $r_{(\widehat{\mathcal{R}})}$, and $s_{(\widehat{\mathcal{R}})}$ mentioned above. The task of evaluating the 4D, $\mathcal{N} = 1$ “Gadget” over the (at most ten or minimum of three) supermultiplet representations is not a terribly daunting task.

On the other hand, as the reduction process injects the images of these 4D, $\mathcal{N} = 1$ supermultiplets into the sea of 36,864 adinkras, the equivalent task of evaluating the analog of the Gadget defined on adinkras amounts to evaluating all 1,358,954,496 matrix elements in a $36,864 \times 36,864$ matrix over the space indexed by (\mathcal{R}) . As shown with the work of [30], modern computer-enabled algorithms permit the explicit evaluation of all matrix elements. The results are encouraging as about 82% of the matrix elements vanish.

Even while the adinkra Gadget of [30] was being proposed, prior work [31] indicated for all adinkras with an even number of colors, there are more similar quantities that can be defined. Thus, the prediction of a “second Gadget” is the subject of this current work. We confirm its existence, and determine all of its 1,358,954,496 matrix elements by two separate methods.

The first approach is an analytical one. It is based on private communications with mathematicians (Charles Doran, Jordan Kostiuk [32], and Yan X. Zhang [33]) who have been investigating the possibility to generalize the Gadget in the work [29]. Their approach suggested a simplification in evaluating Gadgets based on use of the “ ℓ and $\tilde{\ell}$ ” parameters in one of the two methods proposed to calculate the Gadget in [29].

The second chapter reviews the definition of the first Gadget $\mathcal{G}[(\mathcal{R}), (\mathcal{R}')]_{(1)}$, taking particular note of its two distinct forms expressed as (a.) traces over products of matrices and, (b.) as a quadratic form over the “ ℓ and $\tilde{\ell}$ ” parameters defined previously. It is shown how the \mathbb{Z}_2 valued function $\chi_o(\mathcal{R})$ [28] may be used to express the Gadget in the form of a product involving a smaller quadratic form.

In the third chapter, using these analytical expressions relating the two Gadgets we are able to predict the range and frequency of the values of the matrix elements of the second Gadget $\mathcal{G}[(\mathcal{R}), (\mathcal{R}')]_{(2)}$ based on $\chi_o(\mathcal{R})$ and the first Gadget $\mathcal{G}[(\mathcal{R}), (\mathcal{R}')]_{(1)}$ over both the small BC_4 library (introduced in [29]) as well as over all 36,864 values of (\mathcal{R}) .

The fourth chapter presents the results of the calculations for the 1,358,954,496 matrix elements when the second Gadget is evaluated over the small BC_4 library (where it defines as 96×96 matrix) and over the entire range of the representation label (\mathcal{R}) where it is a $36,864 \times 36,864$ matrix. The results are written in the form of frequency tables of the entries of the in the second Gadget as well as by use of the “Summary of the Gadget” holomorphic functions (as introduced in [30]). It turns out that the second Gadget possesses the exact same set of entries whose values equal zero as the first Gadget, possesses some entries that take on the new value of -1 (compared to the first Gadget), and re-arranges the frequencies of the entries of the first Gadget.

The fifth chapter presents the easily access graphical presentation of the results for both the first and second Gadgets considered over the small BC_4 library. This chapter contains scalable pdf images for each Gadget that allows the explicit values of the matrix elements to be determined via a color code scheme.

We next turn in the sixth chapter to the description of three set of codes, the first two written in Python and the final in MATLAB. The MATLAB code was created as a “fast check” for the arguments made for analytical derived results over the small BC_4 library. After agreement was shown here, the Python code was run over both the BC_4 small library as well as over the complete 36,864 values of the entire (\mathcal{R}) library. Agreement was shown for both the small library results as well as the analytically derived results. Finally, the two different Python codes were created independently to act as additional quality checks on the generation of the 2,717,908,992 matrix elements generated for $\mathcal{G}[(\mathcal{R}), (\mathcal{R}')]_{(1)}$ and $\mathcal{G}[(\mathcal{R}), (\mathcal{R}')]_{(2)}$ over the complete range of the 36,864 adinkras.

Our Python codes will be provided free to any interested reader as we support open access research in our domain. This can be provided by making a simple request via e-mail to any of the authors. Alternately, any interested party upon clicking the links at:

(a.) <https://github.com/vkorotkikh/SUSY-Adinkra-Gadget2>, and

(b.) https://github.com/lk11235/SUSY_AdinkraGadget2_parallel

on-line can initiate a download of these codes.

The seventh chapter contains our conclusions.

2 Optimizing The First Gadget

By use of a set of Feynman-like rules, any adinkra representation (\mathcal{R}) leads to a set of $\mathbf{L}_I^{(\mathcal{R})}$ and $\mathbf{R}_I^{(\mathcal{R})}$ matrices that satisfy the ‘‘Garden Algebra’’ conditions,

$$\begin{aligned} (\mathbf{L}_I^{(\mathcal{R})})_{i\hat{j}} (\mathbf{R}_J^{(\mathcal{R})})_{\hat{j}}^k + (\mathbf{L}_J^{(\mathcal{R})})_{i\hat{j}} (\mathbf{R}_I^{(\mathcal{R})})_{\hat{j}}^k &= 2 \delta_{IJ} \delta_i^k, \\ (\mathbf{R}_J^{(\mathcal{R})})_{i\hat{j}} (\mathbf{L}_I^{(\mathcal{R})})_{\hat{j}}^{\hat{k}} + (\mathbf{R}_I^{(\mathcal{R})})_{i\hat{j}} (\mathbf{L}_J^{(\mathcal{R})})_{\hat{j}}^{\hat{k}} &= 2 \delta_{IJ} \delta_i^{\hat{k}}, \\ (\mathbf{R}_I^{(\mathcal{R})})_{\hat{j}}^k \delta_{ik} &= (\mathbf{L}_I^{(\mathcal{R})})_{i\hat{j}}^{\hat{k}} \delta_{\hat{j}\hat{k}}, \end{aligned} \quad (2.1)$$

and for a specified adinkra representation (\mathcal{R}) , these can be used to define two additional sets of matrices. We have given the name of ‘‘bosonic holoraumy matrices’’ and ‘‘fermionic holoraumy matrices,’’ respectively, to these other sets denoted by $\mathbf{V}_{IJ}^{(\mathcal{R})}$ and $\tilde{\mathbf{V}}_{IJ}^{(\mathcal{R})}$ [29], and defined via the equations

$$\begin{aligned} (\mathbf{L}_I^{(\mathcal{R})})_{i\hat{j}} (\mathbf{R}_J^{(\mathcal{R})})_{\hat{j}}^k - (\mathbf{L}_J^{(\mathcal{R})})_{i\hat{j}} (\mathbf{R}_I^{(\mathcal{R})})_{\hat{j}}^k &= i 2 (V_{IJ}^{(\mathcal{R})})_i^k, \\ (\mathbf{R}_I^{(\mathcal{R})})_{i\hat{j}} (\mathbf{L}_J^{(\mathcal{R})})_{\hat{j}}^{\hat{k}} - (\mathbf{R}_J^{(\mathcal{R})})_{i\hat{j}} (\mathbf{L}_I^{(\mathcal{R})})_{\hat{j}}^{\hat{k}} &= i 2 (\tilde{V}_{IJ}^{(\mathcal{R})})_i^{\hat{k}}. \end{aligned} \quad (2.2)$$

Alternately, if we suppress all the matrix indices above, these equations take the forms

$$\begin{aligned} \mathbf{L}_I^{(\mathcal{R})} \mathbf{R}_J^{(\mathcal{R})} + \mathbf{L}_J^{(\mathcal{R})} \mathbf{R}_I^{(\mathcal{R})} &= 2 \delta_{IJ} \mathbf{I}, \\ \mathbf{R}_I^{(\mathcal{R})} \mathbf{L}_J^{(\mathcal{R})} + \mathbf{R}_J^{(\mathcal{R})} \mathbf{L}_I^{(\mathcal{R})} &= 2 \delta_{IJ} \mathbf{I}, \\ \mathbf{L}_I^{(\mathcal{R})} &= [\mathbf{R}_I^{(\mathcal{R})}]^t. \end{aligned} \quad (2.3)$$

(where the superscript t indicates matrix transposition while \mathbf{I} denotes the identity matrix) for the first set and

$$\begin{aligned} \mathbf{L}_I^{(\mathcal{R})} \mathbf{R}_J^{(\mathcal{R})} - \mathbf{L}_J^{(\mathcal{R})} \mathbf{R}_I^{(\mathcal{R})} &= i 2 \mathbf{V}_{IJ}^{(\mathcal{R})}, \\ \mathbf{R}_I^{(\mathcal{R})} \mathbf{L}_J^{(\mathcal{R})} - \mathbf{R}_J^{(\mathcal{R})} \mathbf{L}_I^{(\mathcal{R})} &= i 2 \tilde{\mathbf{V}}_{IJ}^{(\mathcal{R})}, \end{aligned} \quad (2.4)$$

for the second set.

Given two adinkras representations denoted by (\mathcal{R}) and (\mathcal{R}') (which possess N colors, and d open nodes & d closed nodes) along with their associated fermionic holoraumy matrices $\tilde{\mathbf{V}}_{IJ}^{(\mathcal{R})}$ and $\tilde{\mathbf{V}}_{IJ}^{(\mathcal{R}')}$ we form a scalar, ‘‘the gadget value’’ between two representations (\mathcal{R}) and (\mathcal{R}') defined by

$$\mathcal{G}[(\mathcal{R}), (\mathcal{R}')] = \left[\frac{1}{N(N-1) d_{\min}(N)} \right] \sum_{I,J} \text{Tr} \left[\tilde{\mathbf{V}}_{IJ}^{(\mathcal{R})} \tilde{\mathbf{V}}_{IJ}^{(\mathcal{R}')} \right], \quad (2.5)$$

where we exclude the cases of $N = 0, 1$ in (2.5). The function $d_{\min}(N)$ is given by

$$d_{\min}(N) = \begin{cases} 2^{\frac{N-1}{2}}, & N \equiv 1, 7 \pmod{8} \\ 2^{\frac{N}{2}}, & N \equiv 2, 4, 6 \pmod{8} \\ 2^{\frac{N+1}{2}}, & N \equiv 3, 5 \pmod{8} \\ 2^{\frac{N-2}{2}}, & N \equiv 8 \pmod{8} \end{cases}, \quad (2.6)$$

and where only the case of $N = 0$ (i.e. no supersymmetry) in (2.6) is excluded in this definition. It can be seen from (2.6) that for all values of $N > 1$, the number of nodes *must* be a power of two. For every adinkra [3, 15] based on the Coxeter Group BC_4 , the $\mathbf{L}_I^{(\mathcal{R})}$ and $\mathbf{R}_I^{(\mathcal{R})}$ matrices [1, 2] must have four colors ($I = 1, \dots, 4$), four open nodes ($i = 1, \dots, 4$), and four closed nodes ($\hat{k} = 1, \dots, 4$).

As a consequence of (2.1), the $\tilde{V}_{IJ}^{(\mathcal{R})}$ and $\tilde{V}_{IJ}^{(\mathcal{R}')}$ matrices are actually elements of the $\mathfrak{so}(4)$ algebra. Due to this, they may be expanded in the “ α - β ” basis. In other words, the six matrices defined by

$$\begin{aligned}\alpha^{\hat{1}} &= \sigma^2 \otimes \sigma^1, & \alpha^{\hat{2}} &= \mathbf{I}_{2 \times 2} \otimes \sigma^2, & \alpha^{\hat{3}} &= \sigma^2 \otimes \sigma^3, \\ \beta^{\hat{1}} &= \sigma^1 \otimes \sigma^2, & \beta^{\hat{2}} &= \sigma^2 \otimes \mathbf{I}_{2 \times 2}, & \beta^{\hat{3}} &= \sigma^3 \otimes \sigma^2,\end{aligned}\quad (2.7)$$

can be chosen as the basis over which to expand $(\tilde{V}_{IJ}^{(\mathcal{R})})_i^{\hat{k}}$ in the form

$$\tilde{V}_{IJ}^{(\mathcal{R})} = \left[\ell_{IJ}^{(\mathcal{R})\hat{1}} \alpha^{\hat{1}} + \ell_{IJ}^{(\mathcal{R})\hat{2}} \alpha^{\hat{2}} + \ell_{IJ}^{(\mathcal{R})\hat{3}} \alpha^{\hat{3}} \right] + \left[\tilde{\ell}_{IJ}^{(\mathcal{R})\hat{1}} \beta^{\hat{1}} + \tilde{\ell}_{IJ}^{(\mathcal{R})\hat{2}} \beta^{\hat{2}} + \tilde{\ell}_{IJ}^{(\mathcal{R})\hat{3}} \beta^{\hat{3}} \right], \quad (2.8)$$

written in terms of a set of 36 coefficients $\ell_{IJ}^{(\mathcal{R})\hat{1}}, \ell_{IJ}^{(\mathcal{R})\hat{2}}, \ell_{IJ}^{(\mathcal{R})\hat{3}}, \tilde{\ell}_{IJ}^{(\mathcal{R})\hat{1}}, \tilde{\ell}_{IJ}^{(\mathcal{R})\hat{2}},$ and $\tilde{\ell}_{IJ}^{(\mathcal{R})\hat{3}}$.

The values of the “Gadget,” expressed in terms of the ℓ and $\tilde{\ell}$ coefficients, is defined by a quadratic form

$$\begin{aligned}\mathcal{G}[(\mathcal{R}), (\mathcal{R}')]_{\ell} \equiv & \frac{1}{6} \sum_{\hat{a}} \left[\ell_{12}^{(\mathcal{R})\hat{a}} \ell_{12}^{(\mathcal{R}')\hat{a}} + \ell_{13}^{(\mathcal{R})\hat{a}} \ell_{13}^{(\mathcal{R}')\hat{a}} + \ell_{14}^{(\mathcal{R})\hat{a}} \ell_{14}^{(\mathcal{R}')\hat{a}} + \right. \\ & \ell_{23}^{(\mathcal{R})\hat{a}} \ell_{23}^{(\mathcal{R}')\hat{a}} + \ell_{24}^{(\mathcal{R})\hat{a}} \ell_{24}^{(\mathcal{R}')\hat{a}} + \ell_{34}^{(\mathcal{R})\hat{a}} \ell_{34}^{(\mathcal{R}')\hat{a}} + \\ & \tilde{\ell}_{12}^{(\mathcal{R})\hat{a}} \tilde{\ell}_{12}^{(\mathcal{R}')\hat{a}} + \tilde{\ell}_{13}^{(\mathcal{R})\hat{a}} \tilde{\ell}_{13}^{(\mathcal{R}')\hat{a}} + \tilde{\ell}_{14}^{(\mathcal{R})\hat{a}} \tilde{\ell}_{14}^{(\mathcal{R}')\hat{a}} + \\ & \left. \tilde{\ell}_{23}^{(\mathcal{R})\hat{a}} \tilde{\ell}_{23}^{(\mathcal{R}')\hat{a}} + \tilde{\ell}_{24}^{(\mathcal{R})\hat{a}} \tilde{\ell}_{24}^{(\mathcal{R}')\hat{a}} + \tilde{\ell}_{34}^{(\mathcal{R})\hat{a}} \tilde{\ell}_{34}^{(\mathcal{R}')\hat{a}} \right],\end{aligned}\quad (2.9)$$

and necessarily when $(\mathcal{R}) = (\mathcal{R}')$ this is a non-negative quadratic form. Due to this property, an angle between (\mathcal{R}) and (\mathcal{R}') can be defined by

$$\cos \{ \theta[(\mathcal{R}), (\mathcal{R}')]_{\ell} \} = \frac{\mathcal{G}[(\mathcal{R}), (\mathcal{R}')]_{\ell}}{\sqrt{\mathcal{G}[(\mathcal{R}), (\mathcal{R})]_{\ell}} \sqrt{\mathcal{G}[(\mathcal{R}'), (\mathcal{R}')]_{\ell}}}, \quad (2.10)$$

and clearly when the condition

$$\mathcal{G}[(\mathcal{R}), (\mathcal{R})]_{\ell} = 1, \quad (2.11)$$

is met, the Gadget value corresponds directly to the cosine of an angle.

In recent works [32,33], there has been exploited a calculational advantage to using a different form of (2.9) by making note that for all adinkras constructed from elements in BC_4 , the identities

$$\ell_{IJ}^{(\mathcal{R})\hat{a}} = \frac{1}{2} \chi_o(\mathcal{R}) \epsilon^{\text{IJKL}} \ell_{\text{KL}}^{(\mathcal{R})\hat{a}}, \quad \tilde{\ell}_{IJ}^{(\mathcal{R})\hat{a}} = \frac{1}{2} \chi_o(\mathcal{R}) \epsilon^{\text{IJKL}} \tilde{\ell}_{\text{KL}}^{(\mathcal{R})\hat{a}}, \quad (2.12)$$

are valid. In this expression $\chi_o(\mathcal{R})$ is a function (as first identified in the work of [28]) that *only* takes on values of either +1 or -1 for any BC_4 based adinkras. Using this, the result in (2.9) can be expressed as the product of two factors

$$\mathcal{G}[(\mathcal{R}), (\mathcal{R}')]_{\ell} \equiv \frac{1}{6} [1 + \chi_o(\mathcal{R}) \chi_o(\mathcal{R}')] \mathcal{G}[(\mathcal{R}), (\mathcal{R}')]_{\ell}. \quad (2.13)$$

where the second factor $\mathcal{G}[(\mathcal{R}), (\mathcal{R}')]_{\ell}$ takes the explicit form give by

$$\begin{aligned}\mathcal{G}[(\mathcal{R}), (\mathcal{R}')]_{\ell} = & \frac{1}{3} \left\{ \sum_{\hat{a}} \left[\ell_{12}^{(\mathcal{R})\hat{a}} \ell_{12}^{(\mathcal{R}')\hat{a}} + \ell_{13}^{(\mathcal{R})\hat{a}} \ell_{13}^{(\mathcal{R}')\hat{a}} + \ell_{23}^{(\mathcal{R})\hat{a}} \ell_{23}^{(\mathcal{R}')\hat{a}} + \right. \right. \\ & \left. \left. \tilde{\ell}_{12}^{(\mathcal{R})\hat{a}} \tilde{\ell}_{12}^{(\mathcal{R}')\hat{a}} + \tilde{\ell}_{13}^{(\mathcal{R})\hat{a}} \tilde{\ell}_{13}^{(\mathcal{R}')\hat{a}} + \tilde{\ell}_{23}^{(\mathcal{R})\hat{a}} \tilde{\ell}_{23}^{(\mathcal{R}')\hat{a}} \right] \right\},\end{aligned}\quad (2.14)$$

It should be noted that for all adinkras based on BC_4 , either all the $\ell_{IJ}^{(\mathcal{R})\hat{a}}$ or the $\tilde{\ell}_{IJ}^{(\mathcal{R})\hat{a}}$ coefficient vanish and it has been noted [32,33] that the “pre-factor” $1/2 [1 + \chi_o(\mathcal{R}) \chi_o(\mathcal{R}')]_{\ell}$ only takes on values of one and

zero. A final comment about (2.14) is the expression for $G[(\mathcal{R}), (\mathcal{R}')]\ell$ has a form that is identical to that of a Gadget defined on a space of adinkras with three colors.

Direct calculation further has shown [30] that for all minimal BC_4 based valise adinkras, the Gadget only takes on one of four possible values, i. e. $-1/3$, 0 , $1/3$ or 1 . Accordingly, the only angles that occur between the 36,864 BC_4 based adinkras are $\arccos(-1/3)$, $\pi/2$, $\arccos(1/3)$, and 0 . This number of angles, i. e. four, is about 10^{-16} times smaller than if the angles were totally at random distributed among the 36,864 BC_4 based adinkras. Thus, the system of all BC_4 based minimal valise adinkras is highly ordered.

Hereafter, we will call this the “first Gadget” utilizing the convention

$$\mathcal{G}_{(1)}[(\mathcal{R}), (\mathcal{R}')] \equiv \mathcal{G}[(\mathcal{R}), (\mathcal{R}')] \quad , \quad (2.15)$$

and as this name suggests, there is a second Gadget to be defined shortly.

3 Defining The Second Gadget

We can define the “second Gadget” according to the equation

$$\mathcal{G}_{(2)}[(\mathcal{R}), (\mathcal{R}')] = \frac{1}{96} \sum_{I, J, K, L} \epsilon^{IJKL} \text{Tr} \left[\tilde{\mathbf{V}}_{IJ}^{(\mathcal{R})} \tilde{\mathbf{V}}_{KL}^{(\mathcal{R}')} \right] \quad , \quad (3.1)$$

based on the use of the Levi-Civita tensor ϵ^{IJKL} . The evaluation of this over all possible BC_4 related adinkras representations (\mathcal{R}) , and (\mathcal{R}') leads to another set of 1,358,954,496 matrix elements. The existence of multiple numbers of Gadget can be seen as an implication of the work of [31]. There in equation (23) of the work and expression is given for adinkras with arbitrary numbers of colors. The case of four colors is covered in equation (21) of the work. These equations also appeared in the work of [28] where they were presented in equations numbered as (71) and (78) respectively.

We can also note the following identity

$$\begin{aligned} \sum_{I, J, K, L} \epsilon^{IJKL} \text{Tr} \left[\tilde{\mathbf{V}}_{IJ}^{(\mathcal{R})} \tilde{\mathbf{V}}_{KL}^{(\mathcal{R}')} \right] &= 4 \text{Tr} \left[\tilde{\mathbf{V}}_{12}^{(\mathcal{R})} \tilde{\mathbf{V}}_{34}^{(\mathcal{R}')} \right] - 4 \text{Tr} \left[\tilde{\mathbf{V}}_{13}^{(\mathcal{R})} \tilde{\mathbf{V}}_{24}^{(\mathcal{R}')} \right] \\ &+ 4 \text{Tr} \left[\tilde{\mathbf{V}}_{14}^{(\mathcal{R})} \tilde{\mathbf{V}}_{23}^{(\mathcal{R}')} \right] + 4 \text{Tr} \left[\tilde{\mathbf{V}}_{23}^{(\mathcal{R})} \tilde{\mathbf{V}}_{14}^{(\mathcal{R}')} \right] \\ &- 4 \text{Tr} \left[\tilde{\mathbf{V}}_{24}^{(\mathcal{R})} \tilde{\mathbf{V}}_{13}^{(\mathcal{R}')} \right] + 4 \text{Tr} \left[\tilde{\mathbf{V}}_{34}^{(\mathcal{R})} \tilde{\mathbf{V}}_{12}^{(\mathcal{R}')} \right] \quad , \end{aligned} \quad (3.2)$$

which implies further

$$\begin{aligned} \sum_{I, J, K, L} \epsilon^{IJKL} \text{Tr} \left[\tilde{\mathbf{V}}_{IJ}^{(\mathcal{R})} \tilde{\mathbf{V}}_{KL}^{(\mathcal{R}')} \right] &= 16 \sum_{\hat{a}} \left[\ell_{12}^{(\mathcal{R})\hat{a}} \ell_{34}^{(\mathcal{R}')\hat{a}} - \ell_{13}^{(\mathcal{R})\hat{a}} \ell_{24}^{(\mathcal{R}')\hat{a}} + \ell_{14}^{(\mathcal{R})\hat{a}} \ell_{23}^{(\mathcal{R}')\hat{a}} + \right. \\ &\ell_{23}^{(\mathcal{R})\hat{a}} \ell_{14}^{(\mathcal{R}')\hat{a}} - \ell_{24}^{(\mathcal{R})\hat{a}} \ell_{13}^{(\mathcal{R}')\hat{a}} + \ell_{34}^{(\mathcal{R})\hat{a}} \ell_{12}^{(\mathcal{R}')\hat{a}} + \\ &\tilde{\ell}_{12}^{(\mathcal{R})\hat{a}} \tilde{\ell}_{34}^{(\mathcal{R}')\hat{a}} - \tilde{\ell}_{13}^{(\mathcal{R})\hat{a}} \tilde{\ell}_{24}^{(\mathcal{R}')\hat{a}} + \tilde{\ell}_{14}^{(\mathcal{R})\hat{a}} \tilde{\ell}_{23}^{(\mathcal{R}')\hat{a}} + \\ &\left. \tilde{\ell}_{23}^{(\mathcal{R})\hat{a}} \tilde{\ell}_{14}^{(\mathcal{R}')\hat{a}} - \tilde{\ell}_{24}^{(\mathcal{R})\hat{a}} \tilde{\ell}_{13}^{(\mathcal{R}')\hat{a}} + \tilde{\ell}_{34}^{(\mathcal{R})\hat{a}} \tilde{\ell}_{12}^{(\mathcal{R}')\hat{a}} \right] \quad , \end{aligned} \quad (3.3)$$

or more simply the second Gadget takes the alternate form

$$\begin{aligned} \mathcal{G}_{(2)}[(\mathcal{R}), (\mathcal{R}')]_{\ell} &= \frac{1}{6} \sum_{\hat{a}} \left[\ell_{12}^{(\mathcal{R})\hat{a}} \ell_{34}^{(\mathcal{R}')\hat{a}} - \ell_{13}^{(\mathcal{R})\hat{a}} \ell_{24}^{(\mathcal{R}')\hat{a}} + \ell_{14}^{(\mathcal{R})\hat{a}} \ell_{23}^{(\mathcal{R}')\hat{a}} + \right. \\ &\ell_{23}^{(\mathcal{R})\hat{a}} \ell_{14}^{(\mathcal{R}')\hat{a}} - \ell_{24}^{(\mathcal{R})\hat{a}} \ell_{13}^{(\mathcal{R}')\hat{a}} + \ell_{34}^{(\mathcal{R})\hat{a}} \ell_{12}^{(\mathcal{R}')\hat{a}} + \\ &\tilde{\ell}_{12}^{(\mathcal{R})\hat{a}} \tilde{\ell}_{34}^{(\mathcal{R}')\hat{a}} - \tilde{\ell}_{13}^{(\mathcal{R})\hat{a}} \tilde{\ell}_{24}^{(\mathcal{R}')\hat{a}} + \tilde{\ell}_{14}^{(\mathcal{R})\hat{a}} \tilde{\ell}_{23}^{(\mathcal{R}')\hat{a}} + \\ &\left. \tilde{\ell}_{23}^{(\mathcal{R})\hat{a}} \tilde{\ell}_{14}^{(\mathcal{R}')\hat{a}} - \tilde{\ell}_{24}^{(\mathcal{R})\hat{a}} \tilde{\ell}_{13}^{(\mathcal{R}')\hat{a}} + \tilde{\ell}_{34}^{(\mathcal{R})\hat{a}} \tilde{\ell}_{12}^{(\mathcal{R}')\hat{a}} \right] \quad , \end{aligned} \quad (3.4)$$

when expressed in terms of the coefficients $\ell_{IJ}^{(\mathcal{R})\hat{1}}$, $\ell_{IJ}^{(\mathcal{R})\hat{2}}$, $\ell_{IJ}^{(\mathcal{R})\hat{3}}$, $\tilde{\ell}_{IJ}^{(\mathcal{R})\hat{1}}$, $\tilde{\ell}_{IJ}^{(\mathcal{R})\hat{2}}$, and $\tilde{\ell}_{IJ}^{(\mathcal{R})\hat{3}}$. Upon comparing (2.7) to (3.4), it can be seen that the only difference in the two equations is the reversal of the signs for one-third of the terms.

We can also use (2.12) to write (3.4) as the product of two factors

$$\mathcal{G}_{(2)}[(\mathcal{R}), (\mathcal{R}')]_{\ell} = \frac{1}{6} [\chi_o(\mathcal{R}) + \chi_o(\mathcal{R}')] \text{G}[(\mathcal{R}), (\mathcal{R}')]_{\ell} \quad , \quad (3.5)$$

where the second factor is the same as appears in (2.13). We see that when $(\mathcal{R}) = (\mathcal{R}')$ (see the definition of χ_o [28]) we have

$$\mathcal{G}_{(2)}[(\mathcal{R}), (\mathcal{R})] = \chi_o(\mathcal{R}) \quad , \quad (3.6)$$

since the value of the sum taken over any BC_4 related adinkras always yields a factor of three. Thus, the values of χ_o (i. e. “chi-oh”) correspond to the diagonal entries of the second Gadget. The “pre-factor” $1/2 [\chi_o(\mathcal{R}) + \chi_o(\mathcal{R}')]$ only takes on values of minus one, zero, and plus one. Moreover we note that

$$[\chi_o(\mathcal{R}) + \chi_o(\mathcal{R}')] = 0 \leftrightarrow [1 + \chi_o(\mathcal{R})\chi_o(\mathcal{R}')] = 0 \quad , \quad (3.7)$$

so that the zeroes of the two pre-factors are exactly the same pairs of representations.

Since χ_o is not positive definite, $\mathcal{G}_{(2)}[(\mathcal{R}), (\mathcal{R})]$ cannot be used to define a Euclidean metric on the space of adinkras with the property that the angle between two adinkra representations (\mathcal{R}) and (\mathcal{R}') vanishes when $(\mathcal{R}) = (\mathcal{R}')$. The factors of -1 along the diagonal of $\mathcal{G}_{(2)}[(\mathcal{R}), (\mathcal{R}')]$, when considered as a matrix over the 36,864 BC_4 adinkras, prevents the second Gadget from being used in the formula of (2.10) to define a second angle between adinkra representations.

From (2.13) it follows that the identity

$$\frac{1}{2} [1 + \chi_o(\mathcal{R})\chi_o(\mathcal{R}')] \mathcal{G}_{(1)}[(\mathcal{R}), (\mathcal{R}')] = \mathcal{G}_{(1)}[(\mathcal{R}), (\mathcal{R}')] \quad , \quad (3.8)$$

should be valid. Furthermore, since

$$[\chi_o(\mathcal{R}) + \chi_o(\mathcal{R}')] [\chi_o(\mathcal{R}) + \chi_o(\mathcal{R}')] = 2 [1 + \chi_o(\mathcal{R})\chi_o(\mathcal{R}')] \quad , \quad (3.9)$$

it follows the identities

$$[\chi_o(\mathcal{R}) + \chi_o(\mathcal{R}')] \mathcal{G}_{(2)}[(\mathcal{R}), (\mathcal{R}')] = 2 \mathcal{G}_{(1)}[(\mathcal{R}), (\mathcal{R}')] \quad , \quad (3.10)$$

$$\chi_o(\mathcal{R}) \mathcal{G}_{(1)}[(\mathcal{R}), (\mathcal{R}')] = \chi_o(\mathcal{R}') \mathcal{G}_{(1)}[(\mathcal{R}), (\mathcal{R}')] = \mathcal{G}_{(2)}[(\mathcal{R}), (\mathcal{R}')] \quad , \quad (3.11)$$

should be valid. The final line above implies a more symmetrical expression

$$\mathcal{G}_{(2)}[(\mathcal{R}), (\mathcal{R}')] = \frac{1}{2} [\chi_o(\mathcal{R}) + \chi_o(\mathcal{R}')] \mathcal{G}_{(1)}[(\mathcal{R}), (\mathcal{R}')] \quad , \quad (3.12)$$

which informs us that knowledge of the values of $\chi_o(\mathcal{R})$ and $\mathcal{G}_{(1)}[(\mathcal{R}), (\mathcal{R}')]$ are sufficient to determine the values of $\mathcal{G}_{(2)}[(\mathcal{R}), (\mathcal{R}')] over the entirety of the space of BC_4 related adinkras.$

The formula in (3.12) predicts the behavior of the second Gadget without explicit evaluation of (3.1). Since the pre-factor of $\frac{1}{2} [\chi_o(\mathcal{R}) + \chi_o(\mathcal{R}')] only takes on the values of 0 and ± 1 , this implies that $\mathcal{G}_{(2)}[(\mathcal{R}), (\mathcal{R}')] can only take on the values of 0, $\pm 1/3$, and ± 1 . Thus, the second Gadget possesses a set of entries -1 that did not appear in the first Gadget.$$

All the identities in (3.8), (3.10), (3.11), and (3.12), stem from the facts that the two Gadgets, when evaluated on BC_4 based adinkras, take the forms

$$\begin{aligned} \mathcal{G}_{(1)}[(\mathcal{R}), (\mathcal{R}')] &= \frac{1}{2} [1 + \chi_o(\mathcal{R})\chi_o(\mathcal{R}')] G[(\mathcal{R}), (\mathcal{R}')]_{\ell} \quad , \\ \mathcal{G}_{(2)}[(\mathcal{R}), (\mathcal{R}')] &= \frac{1}{2} [\chi_o(\mathcal{R}) + \chi_o(\mathcal{R}')] G[(\mathcal{R}), (\mathcal{R}')]_{\ell} \quad , \end{aligned} \quad (3.13)$$

with the factor of $G[(\mathcal{R}), (\mathcal{R}')]_{\ell}$ being a common one in both definitions. We are also to write one more valid equation of the form

$$\mathcal{G}_{(2)}[(\mathcal{R}), (\mathcal{R}')] = \frac{1}{2} \{ \mathcal{G}_{(2)}[(\mathcal{R}), (\mathcal{R})] + \mathcal{G}_{(2)}[(\mathcal{R}'), (\mathcal{R}')] \} \mathcal{G}_{(1)}[(\mathcal{R}), (\mathcal{R}')] \quad , \quad (3.14)$$

for the matrix elements of the two Gadgets.

4 Results For The Second Gadget

The formula in (3.12), without explicit evaluation of (3.1), also predicts the frequencies with which the non-vanishing elements appear. The frequencies of appearances of $-1/3$, 0 , $1/3$, and 1 in the first Gadget are shown in Table 1

Gadget ₍₁₎ Value	Count
- 1/3	127,401,984
0	1,132,462,080
1/3	84,934,656
1	14,155,776

Table 1: Frequency of Appearance of $\mathcal{G}_{(1)}[(\mathcal{R}), (\mathcal{R}')]]$ Elements

and the formula of (3.12) permits one to predict that the frequency of appearances of ± 1 , $\pm \frac{1}{3}$, and 0 in the second Gadget are given as shown in Table 2.

Gadget ₍₂₎ Value	Count
- 1	7,077,888
- 1/3	106,168,320
0	1,132,462,080
1/3	106,168,320
1	7,077,888

Table 2: Frequency of Appearance of $\mathcal{G}_{(2)}[(\mathcal{R}), (\mathcal{R}')]]$ Elements

In the work of [30] there was introduced a meromorphic “Summary of the Gadget” function for the first Gadget which in light of the introduction of the second Gadget we now write as

$$\begin{aligned}
 \mathcal{S}_{\mathcal{G}(1)}(z) &= \frac{1}{z^{p_1} (z + \frac{1}{3})^{p_2} (z - \frac{1}{3})^{p_3} (z - 1)^{p_4}} , \\
 p_1 &= 1,132,462,080 \quad , \quad p_2 = 127,401,984 \quad , \\
 p_3 &= 84,934,656 \quad , \quad p_4 = 14,155,776 \quad .
 \end{aligned}
 \tag{4.1}$$

This expression has the following properties:

- (a.) the sum of the exponents equals to the square of 36,864, i.e. the rank of the first Gadget matrix,
- (b.) the poles of this function are the only non-vanishing entries that appear in the first Gadget matrix, and
- (c.) the exponent associated with each pole is the multiplicity with which the value of the pole appears in the first Gadget matrix.

Due to the results in Table 2, we can write a similar expression for a meromorphic “Summary of the Gadget” function for the second Gadget

$$\mathcal{S}_{\mathcal{G}(2)}(z) = \frac{1}{z^{p_1} \left(z^2 - \frac{1}{9} \right)^{q_1} (z^2 - 1)^{q_2}} \quad , \quad (4.2)$$

$$q_1 = 106,168,320 \quad , \quad q_2 = 7,077,888 \quad .$$

This expression has the following properties:

- (a.) the sum $p_1 + 2(q_1 + q_2)$ equals to the square of 36,864, i.e. the rank of the second Gadget matrix, and
- (b.) the poles of this function are the only non-vanishing entries that appear in the second Gadget matrix.

5 Visual Graph of The Second Adinkra Gadget Values Over The “Small BC_4 Library”

In the work of [30], we started the demonstration of the structure of the results found for the first Gadget by giving a visual representation over a tiny section of the entries of the full $36,864 \times 36,864$ symmetrical matrix. This tiny section consisted of an examination of only a 96×96 sub-sector of the symmetrical matrix. The 96 adinkra representations contained in the “small BC_4 library” are defined by starting with the Coxeter Group BC_4 , which contains 384 elements, followed by forming tetrads.

In equation (5.6) of that work, six collections of permutations are presented. Each of these collections possesses four permutation elements. Next one takes these collections and multiplies them by the six collections of Boolean Factors shown in Appendix B of [30]. Since each collection of Boolean Factors contains sixteen elements, one ends up with $6 \times 16 = 96$ tetrads. The representation of these 96 tetrads described in terms of their ℓ and $\tilde{\ell}$ values is then given in Appendix C of [30]. Finally, one takes these ℓ and $\tilde{\ell}$ values and substitutes them in (3.4) of this work to calculate the values under the second Gadget. To obtain explicit values, a MATLAB code was created (this will be described in more detail later) to evaluate the Second gadget over the “small BC_4 library.”

We can use the concept of the Summary of the Gadget approach but restricted to the small BC_4 library, and denote by $\mathcal{S}_{\mathcal{G}(1)}^{BC_4}(z)$ and $\mathcal{S}_{\mathcal{G}(2)}^{BC_4}(z)$ for the two Gadgets respectively to find

$$\mathcal{S}_{\mathcal{G}(1)}^{BC_4}(z) = \frac{1}{z^{r_1} (z + \frac{1}{3})^{2r_2} (z - 1)^{2r_3}} \quad , \quad \mathcal{S}_{\mathcal{G}(2)}^{BC_4}(z) = \frac{1}{z^{r_1} (z^2 - \frac{1}{9})^{r_2} (z^2 - 1)^{r_2}} \quad , \quad (5.1)$$

$$r_1 = 4,608 \quad , \quad r_2 = 640 \quad , \quad r_3 = 1,664 \quad ,$$

We note $4,608 + 2(640) + 2(1,664) = 9,216 = (96) \times (96)$. Since the order of the poles at zero are the same for these two expression, this implies the number of zeroes in the two Gadgets is the same. However, the MATLAB code also verified that not only the number of zero entries was the same, it also verified that the locations of the 4,608 zeros occurs in the identically corresponding location of each respective matrix.

A set of visual predictions that follow from (3.12) can be made also. These include:

- (i.) none of the white “pixels” are to be modified,
- (ii.) half of the green “pixels” will be replaced by blue “pixels,”
- (iii.) some red “pixels” are to be replaced by black “pixels,”
- (iv.) the number of red “pixels” must be the same as the number of black “pixels,”
- (v.) the number of green “pixels” must be the same as the number of blue “pixels,” and
- (vi.) on the diagonal only 48 green “pixels” and 48 blue “pixels” appear.

To efficiently show the results for the 9,216 matrix elements over the “small BC_4 library,” we introduce a color key shown in Table 3 relating colors to numerical values. So instead of showing the numerical values, we can use 9,216 “pixels” in their place.






Numerical Value	Color
- 1	
- 1/3	
0	
+ 1/3	
+ 1	

Table 3: Color Key For Matrix Elements

This ⁵ permits the visual representation for all the matrix elements of $\mathcal{G}_{(1)}^{\text{BC}^4}$ shown in Fig. 1,

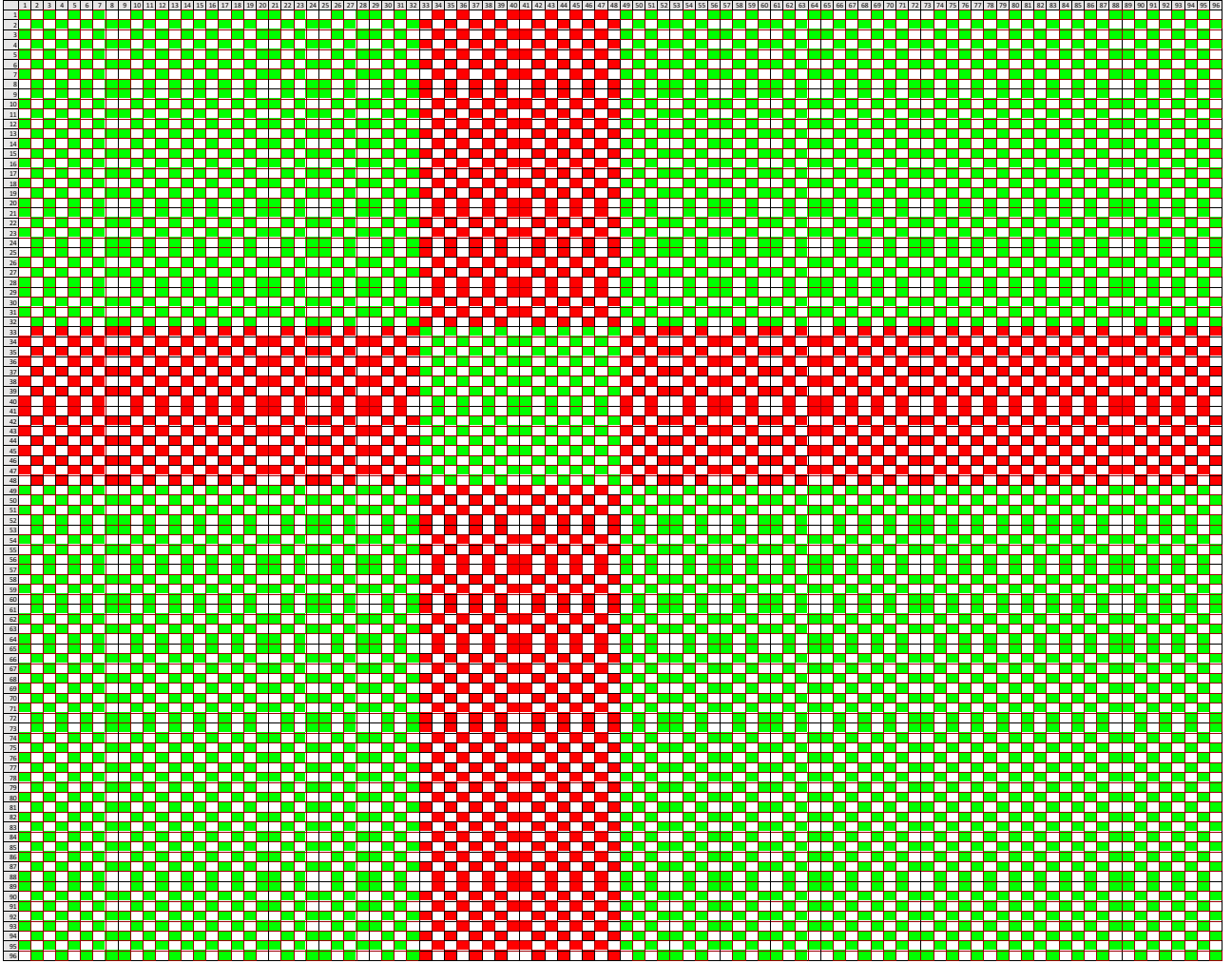


Figure 1: Visual Representation of the Values in First Gadget Adinkra Representation Matrix

⁵ The image shown in Fig. 1 is taken from the text of [30].

and as well to illustrate the visual representation of the all matrix elements of $\mathcal{G}_{(2)}^{\text{BC}_4}$ shown in Fig. 2.

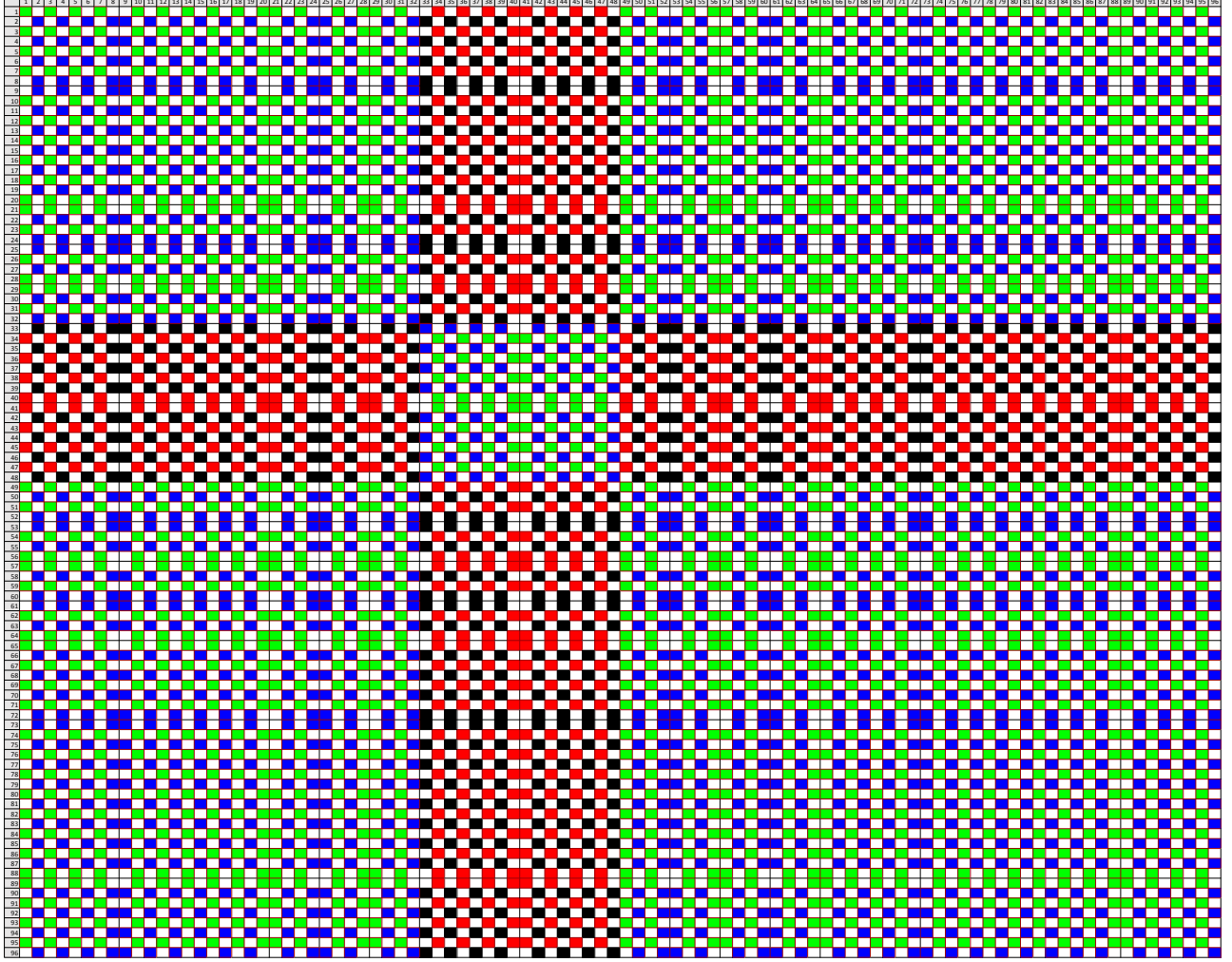


Figure 2: Visual Representation of the Values in Second Gadget Adinkra Representation Matrix

The images in Fig. 1 and Fig. 2 are scalable pdf files in the native format of this document which implies it can be magnified as desired to obtain greater detail.

We can also express the data about the frequency of the various matrix entries that occur in the BC_4 Small Library Count in tabular form. This is shown in Table 3 and Table 4.

Gadget ₍₁₎ Value	BC ₄ Small Library Count
- 1	0
- 1/3	1,280
0	4,608
1/3	0
1	3,328

Table 3: Frequency of Appearance of $\mathcal{G}_{(1)}[(\mathcal{R}), (\mathcal{R}')]]$ Elements Over Small Library

Gadget ₍₂₎ Value	BC ₄ Small Library Count
- 1	1,664
- 1/3	640
0	4,608
1/3	640
1	1,664

Table 4: Frequency of Appearance of $\mathcal{G}_{(2)}[(\mathcal{R}), (\mathcal{R}')]$ Elements Over Small Library

Having verified (3.12) over the 9,216 entries of the small library, we next turn to the issue of evaluating it over the 1,358,954,496 entries of the entirety of BC₄. A discussion of the code used for doing this appears in chapter six.

6 The Codes

6.1 Python Code-I Version

This subsection contains a general description of the Python software code used in explicitly calculating the matrix elements of $\mathcal{G}_{(2)}[(\mathcal{R}), (\mathcal{R}')]]$ over the entirety of 36,864 adinkras as well as for the BC_4 Small Library. The code was written in Python 3.5 and executed using Python version 3.5 but it is also compatible with Python 2.7.

6.1.1 Creating all BC_4 space Adinkras

The Python code builds upon earlier developments done in [30] but with modifications to the code that pertain to the second Gadget calculation as well as new code for increasing calculation speed and saving the results. To speed up the Gadget calculation, multiprocessing feature was added and is utilized within the code. The code also now produces a text output of the results which can be zip compressed for easier distribution of results.

The BC_4 Coxeter group elements are defined by `adinkra_nxn_constructor.py` script which creates the 384 L-matrices. These L-matrices serve as the building blocks of all adinkras, given that any two satisfy conditions of the Garden algebra equations. Once the 384 L-matrices are created, for each L matrix the script builds a list of compatible matrices that satisfy Garden Algebra conditions. Given 384 L-matrices, allowing for all “color permutations” in an adinkra there is a total of 36,864 adinkras with four color, four open node and four close node.

6.1.2 Calculating Holoraumy Matrices

The `fx_vij_holoraumy.py` script is used to calculate the Holoraumy matrices for each one adinkra of the 36,864. This script can calculate the $\tilde{\mathbf{V}}$ Fermionic Holoraumy matrices well as the ℓ and $\tilde{\ell}$ coefficients for $\tilde{\mathbf{V}}$ matrices. The `fermionic_holomats` function generates a set of six $\tilde{\mathbf{V}}$ matrices for any given adinkra.

The `calc_vij_alphabeta` function uses the six $\tilde{\mathbf{V}}$ matrices to calculate the corresponding ℓ and $\tilde{\ell}$ coefficient values. Once the calculation is finished executing the `fx_vij_holoraumy.py` script returns a list (a mutable data structure in Python) of calculated ℓ and $\tilde{\ell}$ coefficients. These coefficients and the $\tilde{\mathbf{V}}$ matrices will be used in second Gadget calculations. The value calculation for the second Gadget is done by the `fx_mpgadgets.py` script. This script utilizes the multiprocessing module available in Python to greatly speed up the Gadget calculation process. The values for the second Gadget can be calculated via two different ways.

First is taking the sum of all traces of $\tilde{\mathbf{V}}$ matrices from any two adinkras. If (\mathcal{R}) and (\mathcal{R}') are any two adinkras from the set of 36,864 then the Gadget II app is defined by the equation (3.1). This is performed in `newgadget_mtraces` and `newgadget_trace` functions. These functions are not multithreaded and only return the Gadget II values to caller. Gadget II can also be calculated by using the ℓ or $\tilde{\ell}$ coefficients of any two (\mathcal{R}) and (\mathcal{R}') adinkras via use of (3.4).

As a check on the consistency of the calculations both methods were used. No differences were found between Gadget II values calculated via the Trace method or the $\tilde{\ell}$ coefficient method.

The advantage to using the $\tilde{\ell}$ coefficients is that it eliminates extensive matrix dot product calculations and instead simplifies each gadget calculation to summing up the 1 and -1. This type of Gadget II calculation method is done in the `mp_gadgetcalc_abonly` function. This function utilizes numpy multiprocessing module to split the Gadget II calculations into multiple threads and can also write the Gadget II values for any adinkra to a text file. It is noticeably different from the original Gadget equation. This makes

the task of calculating all Gadget II values a lengthy process because there are $36,864 \times 36,864$ possible combinations of adinkras which cannot be quickly reduced resulting in a total number of 1,358,954,496 calculations. Even if the same two adinkras are paired in the equation again but the order is reversed this does not guarantee the same Gadget value as opposed to the original Gadget equation.

The original Gadget calculation algorithm took (\mathcal{R}) adinkra from the set 36,864 adinkras and then proceeded to calculate the Gadget value for each $\mathcal{G}_{(2)}(\mathcal{R}, \mathcal{R}')$ pair for n adinkra in set 36,864. A Python multiprocessing module was used in calculating the Gadget II values by breaking up the Gadget II calculation from a single thread into 64 threads. This entailed breaking up the list of 36,864 adinkras into 64 sets so now the (\mathcal{R}) adinkra was paired simultaneously across 64 different threads against 4608 (\mathcal{R}') adinkras in each thread. Gadget II values were tracked and counted in each thread and the final Gadget II values for each (\mathcal{R}) were written to a dedicated flat file.

The results of these Gadget II apps over the entire library of 36,864 adinkras are shown in Table 2.

6.1.3 The \mathbf{BC}_4 Small Library Gadget II

Calculations of Gadget II values for the \mathbf{BC}_4 Small Library are done by using the aforementioned scripts with hardcoded \mathbf{BC}_4 Small Library. The Small Library is defined in `fx.bc4small_libdef.py`. This script calculates all the 96 adinkras and those are then fed into `fx_vij_holoraumy.py` and then `fx_gadgets.py`. The `fx_gadgets.py` is the single threaded version of the `fx_mpgadgets.py` script. Because there is only 9,216 total Gadget II values for Small Library multithreading is not needed.

The results of these Gadget II apps over the small \mathbf{BC}_4 library adinkras are shown in Table 4.

6.2 Python Code-II Version

6.2.1 Building Libraries

We begin by constructing all 384 permutation matrices and 16 binary matrices of size 4×4 , the dimensions required to describe adinkras in the 1D, $N = 4$ space. Then, we construct tetrads of the signed permutation matrices such that each set of four \mathbf{L} -matrices conforms to the rules required of valid adinkras—these tetrads can be treated similar to adjacency matrices in the construction of each adinkra.

After indexing all 36,864 valid adinkras, we build a dictionary that maps each adinkra to its respective permutation and binary matrices, as well as their resultant \mathbf{L} - and \mathbf{R} -matrices. We then iterate over \mathbf{L}_I and \mathbf{R}_J for $I, J = 0, 1, 2, 3$ to make a dictionary mapping our adinkras to their Bosonic Holoraumy matrices (i.e. \mathbf{V} -matrices). Note, we note $(\mathcal{R}) = 1, \dots, 36,864$ and

$$\mathbf{V}_{IJ}^{(\mathcal{R})} = -i\frac{1}{2} \left[\mathbf{L}_I^{(\mathcal{R})} \mathbf{R}_J^{(\mathcal{R})} - \mathbf{L}_J^{(\mathcal{R})} \mathbf{R}_I^{(\mathcal{R})} \right] \quad . \quad (6.1)$$

We can analogously construct a Fermionic Holoraumy matrix (i.e. $(\tilde{\mathbf{V}})$ -matrix) dictionary, since

$$\tilde{\mathbf{V}}_{IJ}^{(\mathcal{R})} = -i\frac{1}{2} \left[\mathbf{R}_I^{(\mathcal{R})} \mathbf{L}_J^{(\mathcal{R})} - \mathbf{R}_J^{(\mathcal{R})} \mathbf{L}_I^{(\mathcal{R})} \right] \quad (6.2)$$

Saving our dictionaries for quick recollection in future runs of our calculation, we modify our code to read our adinkra and matrix libraries from local files, in lieu of recreating our results every run. This sets the foundation for our calculation of the Second Gadget over the whole space of 1D, $N = 4$ adinkras.

6.2.2 Calculating in Python

The calculation of the Second Gadget is executed after recalling our matrix and adinkra libraries, and is carried out over a user-specified range.

We define a function that takes two adinkras as input, “adink1” and “adink2.” The former is given by a for-loop over the specified range of adinkra indices, while the latter is iterated over the the whole space of 36,864 adinkra.

This function, which we denote as “gadgetVV,” explicitly carries out one of the calculations described by 3.1 by iterating over the indices I and J.

Programmatically, this is done in the form of four nested for-loops. While this approach is not ideal for efficiency, it was taken to simplify the original code and aid in collaboration. Calling gadgetVV over all pairs of adink1 and adink2 (where adink1 lay within the user-specified range) effectively calculates all gadget values that involve the adinkra denoted adink1 in the entire 1.3 billion space of gadget values.

Evaluating gadgetVV over all possible (adink1, adink2) pairs takes an unreasonable amount of time, so we took advantage of Python’s support for parallelization. We opted to utilize “multiprocessing,” which is a Python package that “supports spawning processes using an API similar to the threading module” [34]. Again we chose to do this instead of utilizing GPU parallelization or rewriting our code in a parallel-friendlier environment due to collaborative considerations.

From the multiprocessing module, we primarily utilized the Pool object, which offers a “convenient means of parallelizing the execution of a function across multiple input values, distributing the input data across processes (data parallelism)” [34].

This allowed us to submit multiple instances of the gadgetVV function that ran in parallel over all of our desired (adink1, adink2) tuples. By splitting up the whole adinkra space over a farm of 64-core CPUs, and parallelizing Gadget calculations over all 64 cores on each machine, we were able to drastically reduce the computation time.

We also noted that $\text{gadgetVV}(\text{adink1}, \text{adink2}) = \text{gadgetVV}(\text{adink2}, \text{adink1})$, and that $\text{gadgetVV}(\text{adink1}, \text{adink1}) = 0$. Thus by limiting the value of adink2 to the range of indices between adink1 and 36,863, we more than halved our overall set of calculations.

6.3 MATLAB Version

A MATLAB code was written in order to calculate the values of the second Gadget matrix over the small BC_4 library. This code first imports a data file containing the ℓ and $\tilde{\ell}$ coefficients of the small library adinkras, in arrays formatted to match their indices. The superscript indices (\mathcal{R}), ranging from 1 to 96, are identified by the row number of each element in the arrays. The subscript indices IJ, consisting of 12, 13, 14, 23, 24, and 34, are similarly identified by the column number. For each small library coefficient set with given (\mathcal{R}) and IJ indices, only the single nonzero value corresponding to the appropriate a-index is included, in order to reduce redundant computations.

With these arrays imported, the code uses a nested FOR loop to run Equation 3.4 for each combination of two adinkras R and R from the small library. The results, which are the values of the second Gadget over the small library, are then output as a 96×96 matrix. Lastly, the code counts the number of occurrences of each the values 0, 1, -1, $1/3$, and $-1/3$ in the produced matrix.

7 Conclusion

This work gives an explicit proof of the existence of a second Gadget as well as a description of its 1,358,954,496 matrix elements. Libraries of data of the explicit values of the matrix elements of the second Gadget, as well as those of the first Gadget, have been created and are available upon request. The existence of these libraries could be used as a foundation to use “Big Data” approaches to cull knowledge from these of data sets.

An alternate analytical approach involves the continued study of these data sets. Of particular note is the sparse nature of the $\mathcal{G}_{(1)}[(\mathcal{R}), (\mathcal{R}')]$ and $\mathcal{G}_{(2)}[(\mathcal{R}), (\mathcal{R}')]$ libraries with approximately eighty-two percent of their entries being zero. Of the remaining $2 \times (1,358,954,496) \times 18\%$ non-vanishing matrix elements in both libraries together, all take on one of the four values, $\pm 1/3$. or ± 1 . This situation is highly suggestive that an analytical approach to be used for continued progress involves understanding what symmetry realizations are likely hidden within these libraries. The extremely ordered nature of this result suggests the presence of an undiscovered symmetry in the Gadget systems. This is a lesson from the long history of quantum theory...when matrix elements vanish in an orderly fashion, a symmetry is usually the cause. This will be the subject of future effort.

“All thought is reflection.”

- H. M. S. Coxeter

Acknowledgements

L. Kang, D. Kessler and V. Korotkikh would like to acknowledge their participation in the second annual “Brown University Adinkra Math/Phys Hangout” (18-22 Dec. 2017).

Additional acknowledgment is given to Prof. Charles Doran, Prof. Kevin Ida, Prof. Yan X. Zhang, and Dr. Jordan Kostiuk for conversations which stimulated efficient techniques for considerations surrounding Gadgets and adinkras.

We wish to acknowledge the work of Sylvester J. Gates, III for the creation of the 96×96 pixel representation of the matrix elements of the second Gadget over the small BC_4 library.

References

- [1] S. J. Gates Jr., and L. Rana, “A Theory of Spinning Particles for Large N-extended Supersymmetry (I),” *Phys. Lett.* **B352** (1995) 50, arXiv [hep-th:9504025].
- [2] S. J. Gates Jr., and L. Rana, “A Theory of Spinning Particles for Large N-extended Supersymmetry (II),” *ibid. Phys. Lett.* **B369** (1996) 262, arXiv [hep-th:9510151].
- [3] M. Faux, S. J. Gates Jr. “Adinkras: A Graphical Technology for Supersymmetric Representation Theory,” *Phys. Rev.* **D71** (2005) 065002, [hep-th/0408004].
- [4] C. Doran, K. Iga, J. Kostiuk, G. Landweber, and S. Mendez-Diez, “Geometrization of N-extended 1-dimensional supersymmetry algebras, I,” *Adv. Theor. Math. Phys.* **19** (2015) 1043-1113, DOI: 10.4310/ATMP.2015.v19.n5.a4. e-Print: arXiv:1311.3736 [hep-th].
- [5] C. Doran, K. Iga, J. Kostiuk, G. Landweber, and S. Mendez-Diez, “Geometrization of N-Extended 1-Dimensional Supersymmetry Algebras II,” e-Print: arXiv:1610.09983 [hep-th].
- [6] Klein, F. “Vorlesungen ueber das Ikosaeder und die Aufloesung der Gleichungen vom fuenften,” Grade. 1884. Reprinted as Klein, F. *Lectures on the Icosahedron and the Solution of Equations of the Fifth Degree*, 2nd rev. ed. New York: Dover, 1956; Arfken, G. *Mathematical Methods for Physicists*, 3rd ed. Orlando, FL: Academic Press, pp. 184-185 and 239-240, 1985.
- [7] M. Marcolli, and N. Zolman, “Adinkras, Dessins, Origami, and Supersymmetry Spectral Triples,” Jun 14, 2016. 25 pp., e-Print: arXiv:1606.04463 [math-ph].
- [8] Yan X. Zhang, “Adinkras for Mathematicians,” *Transactions of the American Mathematical Society*, Vol. **366**, No. 6, June 2014, Pages 3325-3355 S 0002-9947(2014)06031-5.
- [9] C. F. Doran, K. Iga, and G. Landweber, “An application of Cubical Cohomology to Adinkras and Supersymmetry Representations,” July 2012, 1207.6806, e-Print: arXiv:1207.6806 [hep-th], (unpublished).
- [10] C. F. Doran, M. G. Faux, S. J. Gates, Jr., T. Hübsch, K. M. Iga, and G. D. Landweber, “On Graph-Theoretic Identifications of Adinkras, Supersymmetry Representations and Superfield,” *Int. J. Mod. Phys.* **A22** (2007) 869-930, DOI: 10.1142/S0217751X07035112 e-Print: math-ph/0512016.
- [11] C. F. Doran, M. G. Faux, S. J. Gates, Jr., T. Hübsch, K. M. Iga, G. D. Landweber, and R. L. Miller, “Topology Types of Adinkras and the Corresponding Representations of N-Extended Supersymmetry,” UMDEPP-08-010, SUNY-O-667, e-Print: arXiv:0806.0050 [hep-th].
- [12] C. F. Doran, M. G. Faux, S. J. Gates, Jr., T. Hübsch, K. M. Iga, and G. D. Landweber, “Relating Doubly-Even Error-Correcting Codes, Graphs, and Irreducible Representations of N-Extended Supersymmetry,” UMDEPP-07-012 SUNY-O-663, e-Print: arXiv:0806.0051 [hep-th].
- [13] C. F. Doran, M. G. Faux, S. J. Gates, Jr., T. Hübsch, K. M. Iga, G. D. Landweber, and R. L. Miller, “Codes and Supersymmetry in One Dimension,” *Adv. Theor. Math. Phys.* **15** (2011) 6, 1909-1970; e-Print: arXiv:1108.4124 [hep-th].

- [14] R. Horaud, “A Short Tutorial on Graph Laplacians, Laplacian Embedding, and Spectral Clustering,” 2012 (INRIA), <https://csustan.csustan.edu/~tom/Clustering/GraphLaplacian-tutorial.pdf>.
- [15] B. Bollobás, “Modern Graph Theory,” (1998) Springer-Verlag, Heidelberg, eISBN-13: 978-1461206194, ISBN-13: 978-0387984889.
- [16] J. A. Bondy, and U. S. R. Murty, “Graph Theory,” (2010) Springer-Verlag, Heidelberg, ISBN-13: 978-1849966900, ISBN-10: 1849966907.
- [17] M. Bóna, “Walk Through Combinatorics,” (2011) World Scientific, Hong Kong, ISBN-13: 978-9814335232, ISBN-13: 978-9814460002.
- [18] R. Diestel “Graph Theory,” (2016) Springer-Verlag, Heidelberg, ISBN-13: 978-3662536216, ISBN-13: eISBN 978-3961340057.
- [19] J. Gross, and J. Yellen, “Graph Theory And Its Applications,” (2006) CRC Press, Taylor & Francis Group, LLCoca Raton, FL, ISBN-13: 978-1584885054, ISBN-10: 158488505X.
- [20] A. Tannenbaum, C. Sander, R. Sandhu, L. Zhu, I. Kolesov, E. Reznik, Y. Senbabaoglu, and T. Georgiou, “Graph Curvature and the Robustness of Cancer Networks,”
- [21] A. Barabási, “The network takeover, *Nature Physics* **8** (2012), pp. 14-16.
- [22] I. Chappell, II, S. J. Gates, Jr, and T. Hübsch, “Adinkra (In)Equivalence From Coxeter Group Representations: A Case Study,” *Int. J. Mod. Phys’A* **29** (2014) 06, 1450029 e-Print: arXiv:1210.0478 [hep-th].
- [23] H. S. M. Coxeter, “Discrete groups generated by reflections,” *Ann. Of Math.* **35** (3): 588621, (1934) JSTOR 1968753; N. Bourbaki, *Elements of Mathematics*, Lie Groups and Lie Algebras: Ch. 4-6, (2002) Springer, ISBN 978-3-540-42650-9, Zbl 0983.1700.1
- [24] S. J. Gates, Jr., L. Kang, K. M. Iga, V. Korotkikh, and K. Stiffler, “Generating all 36,864 Four-Color Adinkras via Signed Permutations and Organizing into ℓ - and $\tilde{\ell}$ -Equivalence Classes,” Dec 21, 2017. 28 pp., Brown Univ. preprint BROWN-HET-1721, e-Print: arXiv:1712.07826 [hep-th].
- [25] Yan X. Zhang, “A Unified Enumeration of 1-Dimension Garden Algebras and Valise Adinkras,” Dept. of Mathematics Preprint, San Jose State Univ., Jan 8, 2018, e-Print: arXiv:1801.02678 [math.CO] .
- [26] W. Caldwell, A. N. Diaz, I. Friend, S. J. Gates, Jr., S. Harmalkar, T. Lambert-Brown, D. Lay, K. Martirosova, V. A. Meszaros, M. Omokanwaye, S. Rudman, D. Shin, and A. Vershov, “On the Four Dimensional Holoraumy of the 4D, $\mathcal{N} = 1$ Complex Linear Supermultiplet,” Feb 17, 2017. 27 pp. Univ. of MD preprint # PP-017-020, Brown Univ. preprint # HET-1711, e-Print: arXiv:1702.05453 [hep-th].
- [27] S. J. Gates, Jr., W. D. Linch, III, J. Phillips, “When Superspace Is Not Enough,” Univ. of Md Preprint # UMDEPP-02-054, Caltech Preprint # CALT-68-2387, arXiv [hep-th:0211034], unpublished.
- [28] S. J. Gates, Jr. J. Gonzales, B. MacGregor, J. Parker, R. Polo-Sherk, V.G.J. Rodgers and L. Wassink, “4D, $N = 1$ Supersymmetry Genomics (I),” *JHEP* **0912**, 008 (2009), e-Print: arXiv:0902.3830 [hep-th].

- [29] S. J. Gates, T. Grover, M. D. Miller-Dickson, B. A. Mondal, A. Oskoui, S. Regmi, E. Ross, and R. Shetty, “A Lorentz covariant holonomy-induced gadget from minimal off-shell 4D, $N = 1$ supermultiplets,” JHEP **1511** (2015) 113, e-Print: arXiv:1508.07546 [hep-th].
- [30] S. J. Gates, Jr., F. Guyton, S. Harmalkar, D. S. Kessler, V. Korotkikh, and V. A. Meszaros, “Adinkras From Ordered Quartets of BC_4 Coxeter Group Elements and Regarding 1,358,954,496 Matrix Elements of the Gadget,” JHEP 1706 (2017) 006 DOI: 10.1007/JHEP06(2017)006, e-Print arXiv:1701.00304v5 [hep-th].
- [31] B. L. Douglas, S. J. Gates Jr., L. Segler, and J. B. Wang, “Automorphism Properties and Classification of Adinkras, Advances in Mathematical Physics Volume 2015, Article ID 584542, <http://dx.doi.org/10.1155/2015/584542>
- [32] Charles Doran and Jordan Kostiuk, private communications.
- [33] Yan X. Zhang, private communications.
- [34] P. S. Foundation. “17.2. multiprocessing process-based parallelism python 3.6.4 documentation,” <https://docs.python.org/3.6/library/multiprocessing.html>. (Accessed on 01/04/2018).